Growth of Cu Nanobelt and Ag Belt-Like Materials by Surfactant-Assisted Galvanic Reductions

Ting-Kai Huang,[†] Tzu-Hou Cheng,[†] Ming-Yu Yen,[‡] Wei-Han Hsiao,[†] Lung-Shen Wang,[†] Fu-Rong Chen,[§] Ji-Jung Kai,[§] Chi-Young Lee,[||] and Hsin-Tien Chiu*[,†]

Department of Applied Chemistry, National Chiao Tung University, Hsinchu, Taiwan 30050, Republic of China, Energy and Environment Research Laboratories, Industrial Technology Research Institute, Hsinchu, Taiwan 31040, Republic of China, Department of Engineering and System Science, National Tsing Hua University, Hsinchu, Taiwan 30043, Republic of China, and Center for Nanotechnology, Materials Science and Microsystems, National Tsing Hua University, Hsinchu, Taiwan 30043, Republic of China

Received November 13, 2006. In Final Form: March 1, 2007

We demonstrate the syntheses of single crystalline Cu nanobelt and Ag belt-like materials via CTAC-assisted (CTAC, cetyltrimethylammonium chloride) galvanic reductions. The single crystalline face-centered cubic phase Cu nanobelt was prepared by reacting $CuCl_2$(aq) with Al(s) in an aqueous solution of CTAC and HNO_3. The Cu nanobelt exhibited a high-quality ribbon-like nanostructure with a thickness less than 15 nm, a width of 30−150 nm, and a length up to 10 μm. The belt-like Ag, with a thickness less than 10 nm, a width of 30−100 nm, a length up to 5 μm, and a novel single crystalline 4H structure, was prepared by reacting $AgNO_3$(aq) and Cu(s) in an aqueous solution of CTAC.

Introduction

Nanobelts are interesting one-dimensional materials under intensive investigation.[1−15] There are many reports regarding the syntheses and applications of nanobelts of semiconductors and main group elements.[1−7] On the other hand, transition metal nanobelts are much less reported. The only known example is the preparation of Ni nanobelt by a hydrothermal method and Au nanobelt by a sonochemical method.[8,9] Here, we report a surfactant-assisted synthesis of single crystalline cubic phase 3C Cu nanobelt and hexagonal phase 4H Ag belt-like materials via galvanic reductions of $CuCl_2$(aq) and $AgNO_3$(aq) solutions in the presence of CTAC (cetyltrimethylammonium chloride) by Al(s) and Cu(s), respectively. To our knowledge, these are the first examples of Cu nanobelt and Ag belt-like materials reported to this date. The preparation of 4H Ag is a rare case of controlled growth of this material.[16−18] We expect that the metallic nanobelts and belt-like nanostructures, with metallic conductivity and increased surface area, may find future applications as electrodes in sensing devices,[19,20] as contacts for molecular electronic circuits,[21] in surface-enhanced Raman scattering (SERS) spectroscopy,[22,23] and in metal−polymer composites for electromagnetic interference (EMI) shielding layers.[24]

Experimental Section

Preparation of Cu Nanobelts. $CuCl_2$ (Strem, 0.034 g, 0.25 mmol) was added to a stirring aqueous solution (50 mL) of CTAC (Taiwan Surfactant, 1.78×10^{-3} M) and HNO_3 (SHOWA, 5×10^{-3} M) in a glass vial. Immediately, the mixture turned light blue. The mixture was then placed in a water bath controlled at 290 K. An Al TEM grid (Agar, 200 mesh), cleaned in H_3PO_4(aq) (Riedel-de Haen, 5% wt, 3 mL) for 2 m and rinsed by deionized water, was immersed into this mixture. The reaction was controlled at 290 K without stirring. The Al surface turned dark red gradually. After 24 h, the Al grid was removed and rinsed by deionized water.

Preparation of Ag Belt-like Nanomaterials. The preparation of belt-like Ag was described below. $AgNO_3$ (Fisher, 0.085 g, 0.50 mmol) was added to a stirring aqueous solution of CTAC (3.6×10^{-3} M, 50 mL). Immediately, the mixture turned white and opaque. After the colloidal suspension was stirred for 15 m, the mixture was allowed to stand for 5 m more. Then, a Cu TEM grid (Agar, 300 mesh with lacey carbon film), cleaned in HCl(aq) (TEDIA, 1.0 N, 3 mL) for 3 m and rinsed by deionized water, was immersed into this mixture at room temperature. The Cu surface turned gray gradually. After 10 m, the Cu grid was removed and rinsed by deionized water.

* To whom correspondence should be addressed. E-mail: htchiu@faculty.nctu.edu.tw.

[†] National Chiao Tung University.

[‡] Industrial Technology Research Institute.

[§] Department of Engineering and System Science, National Tsing Hua University.

[||] Center for Nanotechnology, Materials Science and Microsystems, National Tsing Hua University.

(1) Wang, Z. L. *Adv. Mater*. **2003**, *15*, 432.
(2) Pan, Z. W.; Dai, Z. R.; Wang, Z. L. *Science* **2001**, *291*, 1947.
(3) Shi, W. S.; Peng, H. Y.; Wang, N.; Xu, C. P.; Li, L.; Lee, C. S.; Lee, S. T. *J. Am. Chem. Soc.* **2001**, *123*, 11095.
(4) Ma, Y.; Qi, L.; Shen, W.; Ma, J. *Langmuir* **2005**, *21*, 6161.
(5) Cao, X. B.; Xia, Y.; Zhang, S. Y.; Li, F. Q. *Adv. Mater*. **2004**, *16*, 649.
(6) Mo, M.; Zeng, J.; Lin, X.; Yu, W.; Zhang, S.; Qian, Y. *Adv. Mater*. **2002**, *14*, 1658.
(7) Zhang, M.; Wang, Z.; Xi, G.; Ma, D.; Zhang, R.; Qian, Y. *J. Cryst. Growth* **2004**, *268*, 215.
(8) Liu, Z.; Li, S.; Yang, Y.; Peng, S.; Hu, Z.; Qian, Y. *Adv. Mater*. **2003**, *15*, 1946.
(9) Zhang, J. L.; Du, J. M.; Han, B. X.; Liu, Z. M.; Jiang, T.; Zhang, Z. F. *Angew. Chem., Int. Ed*. **2006**, *45*, 1116.
(10) Wang, Y.; Zhang, L.; Meng, G.; Liang, C.; Wang, G.; Sun, S. *Chem. Commmun*. **2001**, *24*, 2632.
(11) Xie, Z.; Wang, Z.; Ke, Y.; Zha, Z.; Jiang, C. *Chem. Lett.* **2003**, *32*, 686.
(12) Sun, Y.; Mayers, B.; Xia, Y. *Nano Lett.* **2003**, *3*, 675.
(13) Law, M.; Sirbuly, D.; Johnson, J.; Goldberger, J.; Saykally, R.; Yang, P. *Science* **2004**, *305*, 1269.
(14) Yan, H.; Justin, J.; Law, M.; Saykally, R.; Yang, P. *Adv. Mater*. **2003**, *15*, 1907.
(15) Law, M.; Kind, H.; Kim, F.; Messer, B.; Yang, P. *Angew. Chem., Int. Ed*. **2002**, *41*, 2405.
(16) Novgorodova, D.; Gorshkov, A.; Mokhov, A.; Vses. Zap. *Mineral Obschch.* **1979**, *108*, 552.
(17) Taneja, P.; Banerjee, R.; Ayyub, P.; Dey, G. K. *Phys. Rev. B* **2001**, *64*, 033405−1.
(18) Liu, X. H.; Luo, J.; Zhu, J. *Nano Lett.* **2006**, *6*, 408.
(19) Zen, J. M.; Chung, H. H.; Kumar, A. S. *Anal. Chem.* **2002**, *74*, 1202.
(20) Zen, J. M.; Chung, H. H.; Kumar, A. S. *Analayst* **2000**, *125*, 1633.
(21) Tour, J. M. *Molecular Electronics: Commercial Insights, Chemistry, Devices, Architecture and Programming*;World Scientific: Singapore, 2003; pp 229−250.
(22) Kneipp, K.; Wang, Y.; Kneipp, H.; Perelman, L. T.; Itzkan, I.; Dasari, R.; Feld, M. S. *Phys. Rev. Lett.* **1997**, *78*, 1667.
(23) Nie, S. M.; Emory, S. R. *Science* **1997**, *275*, 1102.
(24) Bagwell, R. M.; McManaman, J. M.; Wetherhold, R. C. *Compos. Sci. Technol.* **2006**, *66*, 522.

10.1021/la063316e CCC: $37.00
Published on Web 04/14/2007

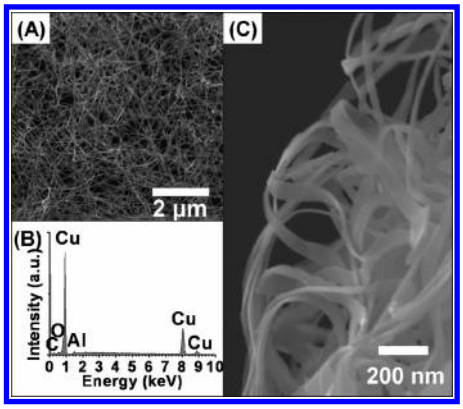

Figure 1. (A) SEM image of Cu nanobelts grown on an Al grid. (B) EDS of the sample in panel A. (C) Enlarged view showing ribbon-like nanostructures.

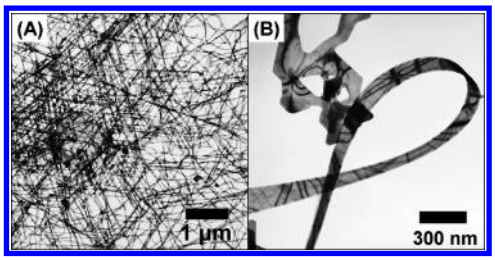

Figure 2. (A) Low and (B) high magnification TEM images of Cu nanobelts.

Characterization. The air-dried samples were investigated by SEM (Hitachi S-4000 at 25 kV and JEOL JSM-6330F at 15 kV), EDS (Oxford Link Pentafet), and TEM (JEOL JEM-2010F at 200 kV and JEOL JEM-4000EX) instruments. The colloid was analyzed by an X-ray diffractometer (XRD, Bruker AXS D8 Advance) and a particle analyzer (Honeywell Microtrac UPA 150).

Results and Discussion

Cu Nanobelts. $CuCl_2$ in an aqueous solution of CTAC and HNO_3 was reduced by an Al transmission electron microscopic (TEM) grid (Agar, 200 mesh) at 290 K. As the reaction progressed, the Al surface turned dark red gradually. An XRD study suggested that 3C Cu was grown on the Al.[25] Figure 1 shows typical SEM and EDS data of the as-prepared product on the TEM grid. Clearly, as shown in Figure 1A, a one-dimensional nanomaterial grows densely across the grid to form an interlacing net. The EDS (Figure 1B) suggests that the product is composed of Cu. In addition, elements in the surrounding, such as C, O, and Al, are observed also. Figure 1C shows an enlarged view of the product, which displays a ribbon-like nanostructure. Generally, the nanobelt has a width of 30−150 nm, a thickness of less than 15 nm, and a length up to 10 μm. Thus, the width-to-thickness and the length-to-width ratios are as high as 10 and 300, respectively. Normally, these characters are maintained across an entire nanobelt. Low magnification TEM images of the nanobelts in Figure 2A display an interlacing net, which is consistent with the observation in Figure 1A. Figure 2B shows characteristic ripple-like images from the strains of belt bending. This feature was frequently observed in TEM studies for thin samples.[1−15] In common cases, selected area ED (SAED) patterns of the nanobelts showed spot patterns revealing single crystalline nature of the samples. They were indexed to be [0,0,1] zone axis of a face-centered-cubic (fcc) structure. The lattice parameter *a* was estimated to be 0.36 nm, close to the reported value of 3C Cu.[25]

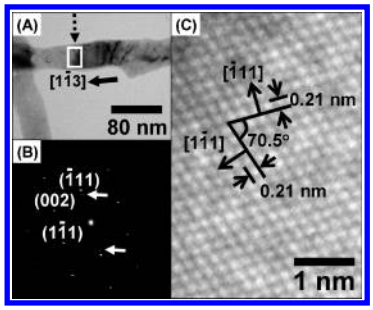

Figure 3. (A) TEM image of Cu nanobelts, (B) [1,1,0] zone SAED, and (C) HRTEM image of the marked rectangular region pointed by the dotted arrow in panel A.

From the pattern, projected growth direction of the nanobelts was determined to be along [1,0,0] direction. In high-resolution TEM (HRTEM) images of the samples, fringes from {2,0,0} planes showing *d* spacing of 0.18 nm were observed. In Figure 3, a set of excellent quality TEM images of a selected nanobelt, examined from a properly adjusted angle, are shown. In Figure 3A, ripple-like contrasts arise from belting are observed again.[1−15] The SAED in Figure 3B displays a spot pattern from the rectangular region marked by a dotted arrow in Figure 3A. This can be indexed to be [1,1,0] zone axis of Cu, with an estimated lattice parameter of 0.36 nm. From the pattern, the apparent growth direction of the nanobelt is determined to be along [1,−1,3] direction. From two tiny dim spots indicated by the arrows in Figure 3B, a *d* spacing of 0.25 nm is estimated. This indicates the presence of a minute quantity of Cu_2O, which has a {1,1,1} spacing distance close to the observed value.[26] The origin is proposed to be some oxidation on the nanobelt surface. Figure 3C presents an HRTEM image from the marked region in Figure 3A. The directions of planes {1,−1,1} and {−1,1,1} are identified from the fringes. The dihedral angle of 70.5° is equal to the theoretical value of an fcc structure. The {1,1,1} *d* spacing is measured to be 0.21 nm, close to the literature value of Cu, 0.208 nm.[25]

We discovered that adding HNO_3 to the reaction mixture is important for the process. Without it, a large amount of aluminum oxide deposit blocked the Al surface and interrupted the Cu growth. The acidic environment probably assists the aluminum oxide dissolution so that active Al metal surface can be exposed. The addition of CATC is also essential to the nanobelt formation. Without the surfactant, only dendridic structures were produced. The physical forms of Al metal did not affect the Cu nanobelt growth much. We tried several types of Al, including powders, foils, and plates. They all showed similar results.

Ag Belt-like Nanomaterials. A similar synthetic approach was applied to prepare Ag belt-like material. An aqueous solution of $AgNO_3$ was added to a stirring CTAC solution. Immediately, the mixture turned white and opaque, indicating the formation of AgCl colloids. Average size of the colloids was measured to be 42 nm by a particle analyzer. Then, after being immersed into the colloidal mixture, the surface of a Cu TEM grid (Agar, 300 mesh with lacey carbon film) turned gray gradually. Figure 4A shows a typical SEM image of the intermingled one-dimensional product on the carbon-coated grid surface. The material grown on the grid is confirmed to be Ag by EDS, as shown in the inset. Figure 4B is an enlarged view of the Ag products. The one-dimensional products do not appear to be cylindrical nanowires with defined diameters. Instead, they show flat and supple belt-like formation. Unlike the Cu nanobelts, the belt-like Ag does not have well-defined facets. Variation in width along the

(25) *Joint Committee for Powder Diffraction (JCPDS) File No. 04-0836*; International Center for Diffraction Data (ICDD), 1982.

(26) *JCPDS File No. 05-0667*; ICDD, 1953.

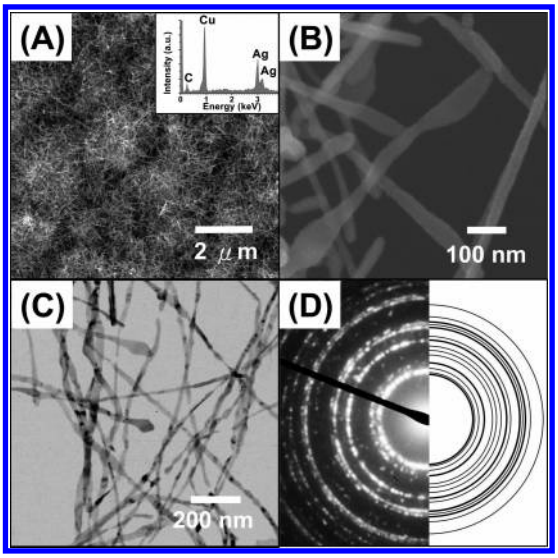

Figure 4. (A) SEM image of belt-like Ag grown on a Cu grid (EDS, inset). (B) Enlarged SEM view showing belt-like nanostructures. (C) TEM image of belt-like Ag. (D) ED pattern of the sample in panel C.

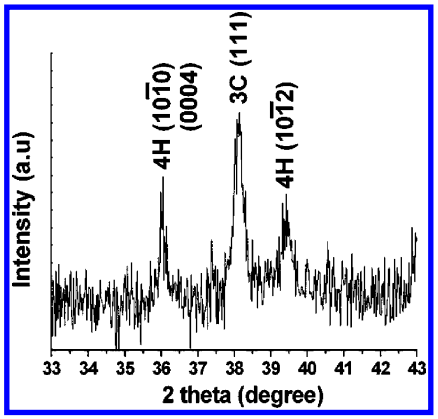

Figure 5. XRD pattern of Ag grown on Cu grid.

longitudinal axis results in varying aspect ratio of width to thickness (w/t). Figure 4C displays a typical TEM image. The highly limpid image suggests that the material is uniform and thin in thickness. In addition, ripple-like contrasts due to strains in thin samples are observed.[1−15] This suggests that the one-dimensional material is belt-like Ag. From a serial of TEM studies, the width, thickness and length of the as-prepared one-dimensional material are estimated to be 20−100 nm, less than 10 nm, and up to 5 μm, respectively. The w/t aspect ratio is estimated in the range of 3 to 13. This is close to the w/t ratio commonly observed for various nanobelts.[1−15] In Figure 4D, an ED pattern from a bunch of belt-like Ag in Figure 4C is shown. The ring pattern, contributed from many orientations of single crystalline belt-like Ag, does not match with the standard diffraction pattern of regular 3C phase Ag.[27] Instead, we discover that the pattern matches the data of a rare hexagonal phase 4H Ag. A simulated diffraction pattern of 4H phase Ag is shown in the right half of Figure 4D.[28]A powder XRD study, shown in Figure 5, reveals that the reflection at $2\theta = 36.0°$ can be assigned to a pair of overlapped planes of 4H Ag {1,0,−1,0} and {0,0,0,4}, while the one at 39.5° to planes of 4H Ag {1,0, −1,2}.[18,28] The averaged lattice parameters *a* and *c*, estimated from the XRD, are 0.291

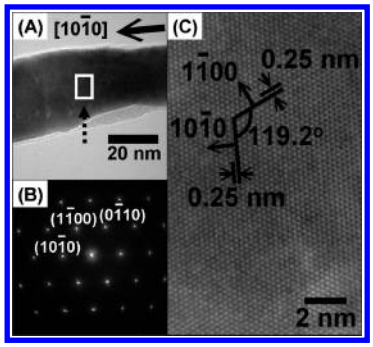

Figure 6. (A) TEM image of a section of belt-like Ag. (B) [0,0,0,1] zone SAED of panel A. (C) HRTEM image of the marked region indicated by a dotted arrow in panel A.

and 1.04 nm, respectively. These are close to the reported values of 4H Ag, $a = 0.2886$ nm and $c = 1.0$ nm.[18,28] In addition, presence of 3C Ag in the bulk material is shown by the peak at $2\theta = 38.1°$, which is assigned to 3C Ag {1,1,1} planes.[27] Based on the relative peak intensities observed for 4H and 3C Ag crystals, we suggest that their quantities in the sample are comparable.

In order to further confirm the formation of 4H Ag, a section of an individual single crystalline Ag, shown in Figure 6A, is studied by ED and HRTEM. The ED shows a hexagonal dot pattern with high 6-fold symmetry in Figure 6B, indicating a single crystalline nature of the sample. The pattern could be indexed either to be [1,1,1] zone axis of a fcc phase or to be [0,0,0,1] zone axis of a hexagonal phase. If the sample were a 3C phase of Ag, the six spots of first order near the beam center should be the reflections from {2,2,0} lattice planes whose spacing is 0.14 nm. However, the *d* spacing estimated from the diffraction pattern in Figure 6B is 0.25 nm. This is too large for the value expected for a regular cubic Ag crystal. On the other hand, the dots of the first order can be perfectly assigned to the reflections from {1,0,−1,0} planes of a hexagonal phase, with a *d* spacing of 0.25 nm. This is in excellent agreement with the value expected for a 4H Ag crystal.[28] As a result, based on the information from Figure 6B, projected growth direction of the belt-like Ag is determined to be along [1,0,−1,0] direction. An HRTEM image in Figure 6C distinctly shows fringes from the area marked by a dotted arrow in Figure 6A. The directions of two sets of planes {1,−1,0,0} and {1,0,−1,0} are identified, showing a dihedral angle of 119.2°. This is close to the theoretical value of 4H Ag, 120°. The *d* spacing of the planes are measured to be ca. 0.25 nm, equal to the value expected for 4H Ag.[28]

In addition to thin belt-like structures, Figure 7 shows that densely packed Ag crystals and wires are found near the Ag/Cu interface. ED studies of the crystals near the Ag/Cu interface shows that the area is mainly composed of cubic phase Ag. These examples suggest that the growth of 4H belt-like Ag is highly sensitive to variables in the environment. Successful fabrication of the material depends on a critical combination of surfactant and reactant concentrations, reaction time, temperature, stirring rate and supplier of Cu. The observation parallels the recent study of 4H Ag nanowires fabricated by AAO-assisted electrochemical deposition.[18]

Proposed Growth Mechanism. The preparation of both Cu nanobelt and Ag belt-like materials are dependent on the presence of CTAC. Without it, the uncontrolled growths produce dendridic structures.[30−33] A generalized CTAC assisted nanobelt growth

(27) *JCPDS File No. 04-0783*; ICDD, 1982.
(28) *JCPDS File No. 87-0598*; ICDD, 1979.
(29) Tsai, J. S.; Chen, F. R.; Kai, J. J.; Chen, C. C.; Huang, R. T.; Wang, M. S.; Huang, G. C.; Guo, G. G.; Yu, M. U. *J. Appl. Phys.* **2004**, *95*, 2015.
(30) Ben-Jacob, E.; Garik, P. *Nature* **1990**, *343*, 523.
(31) Shin, H. C.; Dong, J.; Liu, M. *Adv. Mater.* **2003**, *15*, 1610.
(32) Wang, S.; Xin, H. *J. Phys. Chem. B* **2000**, *104*, 5681.
(33) Ma, Y.; Che, C. M.; Chao, H. Y.; Zhou, X.; Chan, W. H.; Shen, J. *Adv. Mater.* **1999**, *11*, 850.

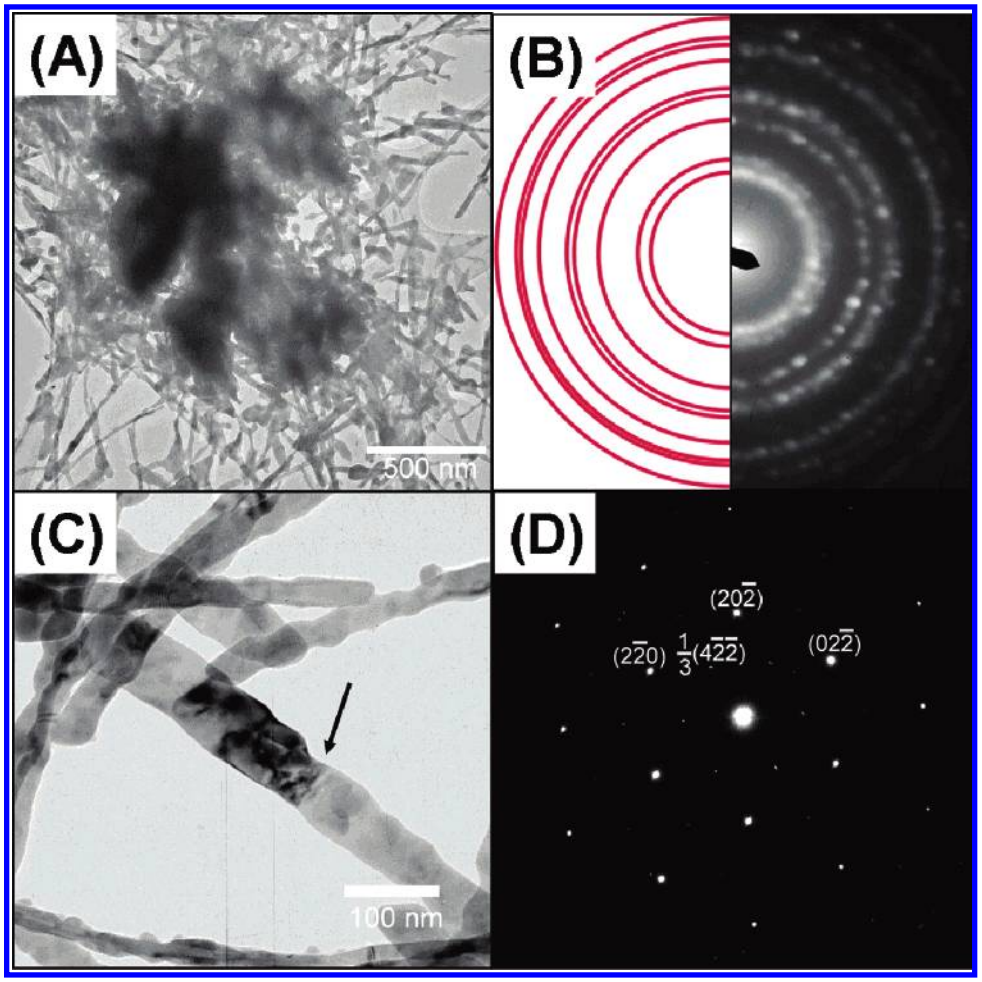

Figure 7. (A) TEM image and (B) ED pattern of a group of crystals. (C) TEM image of wire-like Ag and (D) SAED from a 75 nm diameter wire pointed by the arrow in panel C. The area shows a fundamental [1,1,1] zone cubic pattern. Tiny superlattice diffraction spots could be ascribed to the forbidden 1/3{422} reflections. Vacancy ordering superstructure, surface step and double position twin in a thin fcc sample would give rise to the diffraction pattern.[29]

is presented in Scheme 1 to describe the overall growth process. Galvanic reduction of $Cu^{2+}(aq)$ by more active Al(s) to form Cu nanobelts is described as an example. The $Cu^{2+}(aq)$ ions are reduced and then nucleate into Cu metal on the Al surface. The reaction is spontaneous due to a positive redox potential $E° = 2.00$ V, for the reaction $3Cu^{2+}(aq) + 2Al(s) \rightarrow 3Cu(s) + 2Al^{3+}(aq)$.[34] CTAC molecules probably adsorb selectively on two crystallographically opposite facets of a Cu seed to form a bilayer interface structure.[35,36] Through the ionic ends of the surfactant molecules, one side of the CTAC bilayer binds to the Cu surface while the other side interfaces with the aqueous medium. Between two ionic sides, the aliphatic chains form an inner nonpolar sheet. This specific arrangement restricts the deposition of Cu atoms on the CTAC passivated facets. Consequently, the Cu crystal grows within the CTAC bilayer constructed soft template and develops into a nanobelt.

Apparently, the growth of belt-like Ag can be rationalized by the galvanic reaction, $2Ag^{+}(aq) + Cu(s) \rightarrow 2Ag(s) + Cu^{2+}(aq) E° = 0.46$ V.[34] However, the process is more complicated than it appears. In the studies, we discovered that upon mixing, $Ag^{+}(aq)$ ions combined with $Cl^{-}(aq)$ from CTAC molecules to form AgCl(s) colloids, probably covered by a bilayer shell of CTAC molecules. Since the reaction $2AgCl(s) + Cu(s) \rightarrow 2Ag(s) + Cu^{2+}(aq) + 2Cl^{-}(aq) E° = -0.12$ V is not thermodynamically favored, the growth of Ag cannot proceed via this route.[34] The growth cannot just proceed via the reaction $2Ag^{+}(aq) + Cu(s) \rightarrow 2Ag(s) + Cu^{2+}(aq)$ without CTAC either because this reaction alone did not produce the belt-like structure. On the other hand, illumination during the experiments was found to be important. The belt-like Ag grew only with some illumination, for example, common fluorescent room light. In experiments carried out in darkness, we did not observe belt-like Ag growth at all. Only sparsely dispersed clusters with irregular shapes were observed on Cu surface. Since it is known that AgCl(s) can be reduced to Ag(s) by light,[37] we suggest that nucleation of the belt-like Ag growth was initiated photochemically rather than electrochemically. We propose that Ag seeds enclosed within a bilayer shell of CTAC were generated photochemically. As a result, the CTAC shell acted as a soft template that passivated Ag and restricted further deposition of Ag atoms on them. This might direct Ag atoms, formed from the galvanic reduction $2Ag^{+}(aq) + Cu(s) \rightarrow 2Ag(s) + Cu^{2+}(aq)$, to grow only on the exposed sites, as shown in Scheme 1. Controlling the initial mixing of CTAC and $AgNO_3$ in solution is also important. We discover that both shortened and prolonged stirring of the $Ag^{+}(aq)$/CTAC mixture before the immersion of Cu grids decrease belt-like Ag yields significantly. This resulted in the formation of more irregularly shaped Ag particles. It appears that when the mixing

(34) Bard, A. J.; Faulkner, L. R. *Electrochemical Methods: Fundamentals and Applications*; John Wiley & Sons: New York, 1980.
(35) Gao, J.; Bender, C. M.; Murphy, C. J. *Langmuir* **2003**, *19*, 9065.
(36) Nikoobakht, B.; El-Sayed, M. A. *Langmuir* **2001**, *17*, 6368.
(37) Zayat, M.; Einot, D.; Reisfeld, R. *J. Sol−Gel Sci. Technol.* **1997**, *10*, 67.

Scheme 1. Proposed Growth Mechanism of Cu Nanobelt and Ag Belt-like Materials

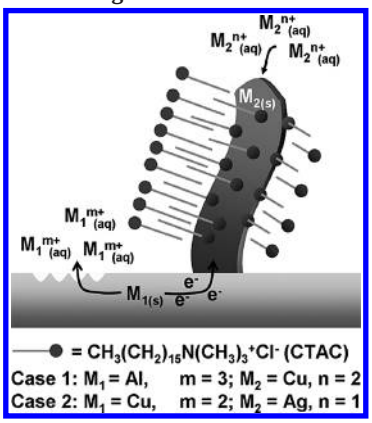

time is shortened, there are not enough photochemically generated Ag seeds for the growth of belt-like Ag. This might result in uncontrolled reduction of Ag^+(aq) on nonselective metal surfaces and lead to isotropic growth of featureless Ag particles. On the other hand, prolonged stirring of the Ag^+(aq)/CTAC mixture would consume a significant portion of the surfactant to form AgCl(s) since the molarity of Ag^+(aq) was several times more than that of CTAC. This decreases the amount of CTAC available to wrap and to shape the growing Ag crystals. Consequently, the CTAC-assisted growth of belt-like Ag is hampered. Instead, the density of Ag particles from uncontrolled growth increases. The reason why 4H Ag is favored under the experimental condition is rationalized below. Apparently, ultra-thin Ag crystals stabilized by the CTAC bilayer shell prefer this unusual hexagonal structure while thick samples exhibit thermodynamically favored cubic phase. This observation agrees with the report that ultra-small Ag crystals can induce hexagonal phase stabilization.[17,18] We suggest that for nanoparticles, surface strains are accommodated by introducing stacking faults that enhance 4H Ag development. In literature, it is found that Ag has extremely low stacking fault energy among several transition metals.[38,39] For large particles, contribution from the surface strains reduces so that growth of 3C Ag is favored.

Conclusion

In summary, we have demonstrated the first time that Cu nanobelt and Ag belt-like materials can be grown via simple galvanic reductions of the corresponding metal ions by active metals in the presence of CTAC in aqueous solutions. There are important differences between the growths of two metals. While the Cu nanobelt can be grown under less restricted conditions, successful fabrication of the belt-like 4H Ag depends on a critical combination of many factors in the environment. This probably is the reason why 4H Ag is rarely observed.[17,18] Application of the synthetic strategy to fabricate nanobelts of other transition metals is underway.

Acknowledgment. We thank the National Science Council and the Ministry of Education of Taiwan, the Republic of China for financial support.

Supporting Information Available: XRD, SEM, TEM, ED and particle size distribution data. This material is available free of charge via the Internet at http://pubs.acs.org.

LA063316E

(38) Meyer, R.; Lewis, L. *J. Phys. Rev. B* **2002**, *66*, 052106−1.
(39) Murr, L. E. *Interfacial Phenomena in Metals and Alloys*; Addison Wesley: London, 1975.